Lowest-energy endohedral fullerene structures of Si_N ($30 \leqslant N \leqslant 39$) clusters by density functional calculations

Li Ma,[1] Jijun Zhao,[2,*] Jianguang Wang,[1] Baolin Wang,[1] and Guanghou Wang[1]
[1]*National Laboratory of Solid State Microstructures and Department of Physics, Nanjing University, Nanjing 210093, People's Republic of China*
[2]*State Key Laboratory of Materials Modification by Laser, Electron, and Ion Beams & College of Advanced Science and Technology, Dalian University of Technology, Dalian 116023, People's Republic of China*
(Received 7 November 2005; published 16 June 2006)

The endohedral fullerene structures of medium-sized Si_N ($30 \leqslant N \leqslant 39$) clusters have been studied using the density functional theory (DFT) with gradient correction. For each cluster size, fullerene cages with different topologies and those filled by a different number of atoms were constructed. These cage isomers were then optimized by DFT-based molecular dynamic relaxations followed by numerical optimization. Compared with recent theoretical calculations [S. Yoo, J. J. Zhao, J. L. Wang, and X. C. Zeng, J. Am. Chem. Soc. **126**, 13845 (2004)], the energies of the lowest-energy fullerene cage structures obtained here are lower for most clusters. In particular, the optimal filling and/or cage combination ratios for Si_{37} and Si_{38} were found to be $Si_5@Si_{32}$ and $Si_6@Si_{32}$, different from the previously proposed ones ($Si_3@Si_{34}$ and $Si_4@Si_{34}$).

DOI: 10.1103/PhysRevA.73.063203 PACS number(s): 36.40.Mr, 61.46.−w, 61.48.+c

Silicon clusters are of great interest and importance from both fundamental and technological points of view. The geometric structures of small silicon clusters have been extensively studied and well established by experimental and theoretical studies [1]. Except for $N=5$, the geometric structures of these clusters for $N<8$ have been confirmed by anion photoelectron spectroscopy of gas-phase clusters [2], or Raman [3] and infrared [4] measurements on matrix-isolated clusters. The geometric structures of small Si_N clusters are far from fragments of a bulk diamond lattice [5,6]. As the cluster size is sufficiently large, it is natural to expect that the silicon clusters would possess a bulklike diamond structure with a reconstructed surface. Thus, understanding the structural evolution with cluster size and exploring the transition towards diamondlike structure are very important issues in the study of silicon clusters and nanostructures. As the bridge between small clusters and nanocrystallines (quantum dots), the medium-sized Si_N ($N \approx 20-100$) clusters have attracted great attention [7–22].

In cluster physics, determining the global minima structures of a cluster is a very challenging problem due to the numerous structural isomers on the potential energy surface (PES). When the cluster size increases, it becomes much more difficult to locate the lowest-energy structure in theoretical studies because the number of the local minimum on the PES increases exponentially. Several global optimization methods such as genetic algorithm [7,21], basin-hopping techniques [22], and "big bang" methods [8], have been employed for the medium-sized Si_N clusters with $N \approx 11-30$. These studies indicated that prolate supercluster structures using tricapped triangular prisms as building blocks are formed for Si_N with $N \approx 15-25$, and that the transition from the prolate to more-spherical configurations occurs at the size range of $N \approx 25-30$. An experimental measurement of ionic mobility of medium-sized Si_N clusters [23] also reveals such a structural transition around $N \approx 25-30$. Above the transition size, most of the cluster properties such as binding energies [24,25], ionization potentials [26], photoelectron spectra [27], and chemical reactivity [28] exhibit smooth size-dependent behavior in experiments. These results imply that the structures of the medium-sized silicon clusters with $N \geqslant 30$ might follow some generic growth pattern. In other words, an addition of one more atom will not induce dramatic structural reconstruction of the medium-sized clusters.

On analogy to the fullerene cages of carbon clusters [1], silicon fullerene cages have been considered in previous studies [9–12]. But the hollow silicon cages were found to be unstable because the valence orbitals of silicon atoms cannot form sp^2 hybridization like carbon. To saturate the dangling bonds of the silicon fullerene surface and stabilize the silicon fullerene cages, some additional atoms are needed to fill inside the cage and form sp^3 hybridization. Based on such consideration, a number of "handmade" endohedral fullerene cages have been constructed for the medium-sized silicon clusters (e.g., Si_{33}, Si_{36}, Si_{39}, Si_{40}, and Si_{45}) [13–18]. However, due to the complexity of the PES, there was no unbiased global optimization of the Si_N ($N \geqslant 30$) clusters to support the guess of endohedral fullerene cages and to determine the optimal filling and/or cage ratio until recent works by Yoo, Zhao, and co-workers [19,20]. From the global search using genetic algorithm (GA) incorporated with a tight-binding (TB) model, endohedral fullerene cages were confirmed to be energetic favorable structural patterns for Si_N ($N=27-40$, 45, and 50) [19,20]. A biased search using a basin-hopping algorithm at a level of density function theory (DFT) was performed to further optimize the lowest-energy structures for Si_N ($N=27-39$) [20]. However, in those previous studies [19,20], the energetically favorable outer fullerene cages and the optimal filling and/or cage combination for the endohedral cages were obtained at a semiempirical TB level, which could be further improved by high-level DFT computations. To further search the lowest-energy endohedral silicon cages within the structural pattern of filled

*Corresponding author. Email address: zhaojj@dlut.edu.cn

fullerenes cages, in this work we examined a number of possible endohedral cages for Si_N in the size range $30 \leqslant N \leqslant 39$ using DFT calculations. For most cluster sizes, new endohedral cages with lower energies were found. The optimal filling and/or cage ratios are discussed and compared with previously proposed empirical rules.

In this work, endohedral fullerene cages of different topologies and with different filling and/or cage ratios were constructed for Si_N ($30 \leqslant N \leqslant 39$). The coordinates of outer silicon fullerene cages were directly taken from those for carbon fullerenes in the fullerene Structure Library [29] and rescaled by a factor of 1.65. For each size of an outer fullerene cage, we consider all possible topologies, that is, from two isomers for 28-atoms fullerene to seven isomers for the 34-atoms fullerene. Afterwards, a suitable amount of silicon atoms are uniformly filled into the hollow silicon cages [18]. These handmade filled fullerene cages were optimized by a two-step strategy. First, the initial structures were relaxed by DFT-based molecular dynamics (MD) using a plane-wave pseudopotential technique implemented in a CASTEP package [30]. Ultrasoft pseudopotential for ion-electron interaction and a 100 eV cutoff of a plane-wave basis set were adopted in the CASTEP calculations. To ensure the systems reaching the equilibrium structures, we took 5 ps or 4000 steps in the MD relaxation. After the MD relaxation, these structural isomers were further optimized using the all-electron DFT program (DMol) [31] with a double numerical basis including *d*-polarization function (DND) [31]. In the DMol calculations, self-consistent field calculations were done with a convergence criterion of 10^{-6} Hartree on the total energy, and the structures were fully optimized without any symmetry constraint with a convergence criterion of 0.002 Hartree/Å on the forces. In both optimization steps (CASTEP and DMol calculations), the exchange-correlation interaction was treated within the generalized gradient approximation (GGA) of the Perdew, Burke and Enzerhof (PBE) functional [32]. The accuracy of the present all-electron PBE computational scheme implemented in DMol has been validated by benchmark calculations on the silicon dimer and the bulk solid in a previous work [18]. For comparison, the lowest-energy configurations obtained for Si_N ($30 \leqslant N \leqslant 39$) in Ref. [20] were also computed.

Using the optimization approach described above, we have examined a number of structural isomers for each size of Si_N ($30 \leqslant N \leqslant 39$) clusters by considering different possible combinations of outer fullerene cages and endohedral filling atoms. For example, the number of isomers increases from 3 for Si_{30} to 12 for Si_{38}. The lowest-energy endohedral fullerenes obtained from this work [denoted as (a)] are shown in Fig. 1, along with the lowest-energy configurations given in Ref. [20] [denoted as (*R*)]. The relative energy differences between these two types of structural isomers are also presented in Fig. 1. The filling and/or cage combination, the symmetry for the original carbon fullerene cage, the binding energies, and the highest occupied molecular orbital–lowest unoccupied molecular orbital (HOMO-LUMO) gaps for these lowest-energy endohedral fullerene structures from previous work [20] and from present calculations are summarized in Table I.

From Fig. 1 and Table I, one can see clearly that the

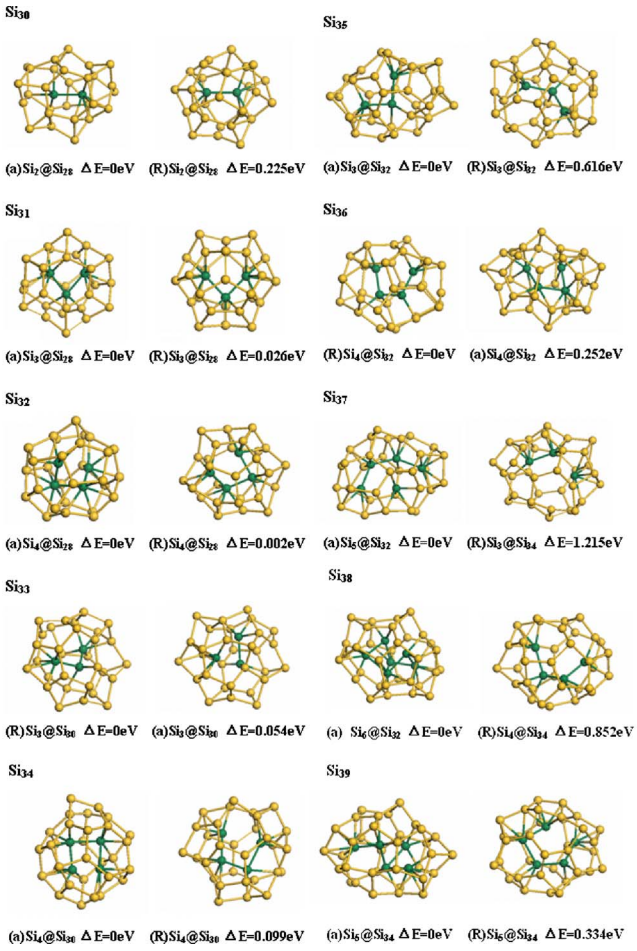

FIG. 1. (Color online) The lowest-energy endohedral fullerene structures from this work [denoted as (a)] and obtained in Ref. [20] [denoted as (*R*)] for medium-sized Si_N ($30 \leqslant N \leqslant 39$) clusters. The interior filling atoms are highlighted.

optimal endohedral fullerenes obtained from present calculations usually have lower total energy or higher binding energy than those from previous calculations [20]. The two exceptional cases are Si_{33} and Si_{36}, where the present total energies for Si_{33} and Si_{36} [33(a) and 36(a) in Fig. 1] are 0.054 and 0.252 eV higher than those from previous calculations [33(*R*) and 36(*R*) in Fig. 1], respectively. These results indicate that a careful examination of the endohedral fullerene cages by considering all the possibilities and optimizing the candidate configurations using the first-principles DFT method is necessary to find the lowest-energy structures within this structural pattern.

We now discuss the lowest-energy endohedral fullerene structures in terms of the filling and/or cage combinations and the outer fullerene cages. As shown in Table I, for most cluster sizes, we obtained the same optimal filling and/or cage ratio as previous work [20], whereas different optimal filling and/or cage combinations were found for Si_{37} and Si_{38}. The present calculations predict the lowest-energy endohedral fullerene as $Si_5@Si_{32}$ and $Si_6@Si_{32}$, while they are $Si_3@Si_{34}$ and $Si_4@Si_{34}$, respectively, in Ref. [20]. The energies for the lowest-energy configuration of Si_{37} and Si_{38} from present calculations are 1.215 and 0.852 eV lower than previous results, respectively.

TABLE I. Optimal filling and/or cage combination ($Si_m@Si_n$), binding energy (E_b) per atom, average coordination number (CN), HOMO-LUMO gap for the lowest-energy structures from this work, and Ref. [20]. The symmetries for the original cages taken from carbon fullerenes are also presented in parentheses for comparison. The average CN was calculated using a 2.65 Å cutoff.

	This work				Ref. [20]			
Si_N	$Si_m@Si_n$	E_b (eV/atom)	CN	Gap (eV)	$Si_m@Si_n$	E_b (eV/atom)	CN	Gap (eV)
Si_{30}	$Si_2@Si_{28}(D_2)$	3.796	3.53	0.795	$Si_2@Si_{28}(T_d)$	3.789	3.47	0.737
Si_{31}	$Si_3@Si_{28}(T_d)$	3.816	3.74	0.963	$Si_3@Si_{28}(T_d)$	3.815	3.81	0.570
Si_{32}	$Si_4@Si_{28}(T_d)$	3.823	3.88	0.357	$Si_4@Si_{28}(T_d)$	3.823	3.88	0.291
Si_{33}	$Si_3@Si_{30}(C_{2v})$	3.823	3.58	0.462	$Si_3@Si_{30}(C_{2v})$	3.824	3.58	0.572
Si_{34}	$Si_4@Si_{30}(C_{2v})$	3.827	3.82	0.574	$Si_4@Si_{30}(C_{2v})$	3.824	3.76	0.473
Si_{35}	$Si_3@Si_{32}(C_2)$	3.831	3.54	0.604	$Si_3@Si_{32}(D_3)$	3.814	3.43	0.463
Si_{36}	$Si_4@Si_{32}(D_{3d})$	3.861	3.89	0.668	$Si_4@Si_{32}(D_3)$	3.868	3.56	0.670
Si_{37}	$Si_5@Si_{32}(C_2)$	3.867	4.00	0.659	$Si_3@Si_{34}(C_2)$	3.840	3.57	0.598
Si_{38}	$Si_6@Si_{32}(D_3)$	3.875	3.84	0.720	$Si_4@Si_{34}(C_2)$	3.853	3.63	0.656
Si_{39}	$Si_5@Si_{34}(C_s)$	3.882	3.79	0.787	$Si_5@Si_{34}(C_2)$	3.873	3.69	0.487

For Si_{30}, Si_{31}, and Si_{32}, the optimal outer fullerene cages are Si_{28} from both previous and present calculations. Previous calculations [20] predicted that the original carbon fullerene cage should have T_d symmetry, while our results show a transition from a D_2 to a T_d fullerene cage between Si_{30} and Si_{31}. For Si_{33} and Si_{34}, both previous and present calculations obtained the same outer fullerene cage, which originally has C_{2v} symmetry. In the size region between Si_{35} and Si_{38}, we found that the outer fullerene cages are all Si_{32}, with different point group symmetries (C_2, D_3, D_{3d}) for the original carbon fullerene cage. Previous calculations predicted an increase of outer fullerene cages from Si_{32} to Si_{34} at Si_{37}, while our present calculations indicate that such an increase occurs at Si_{39}. We also analyzed the structural differences between the present and the previous [20] results. For the endohedral Si atoms, the Si-Si bond lengths are shorter in the present structures than those in the previous structures [20]. In Table I, we included the average coordination numbers (CN) calculated for these two sets of configurations. The average CN for all of these endohedral silicon fullerenes are between 3.5 and 4.0. The average CN for our present structure is usually higher than those in Ref. [20].

The HOMO-LUMO gaps of the lowest-energy endohedral fullerene structures and the previous structures [20] are also given in Table I. Except for Si_{33} and Si_{36}, all the other gaps for the present obtained structures are larger than those of the previous structures, consistent with the energy difference between present and previous structures. Started from Si_{32}, the electronic gap gradually increases with cluster size. Experimentally, it was found that the electronic properties of clusters such as ionization potentials [26] and photoelectron spectra [27] exhibit smooth size-dependent behavior.

Except for the structural patterns considered above, there have been other patterns. For example, Pan and Ramakrishna [15] proposed endohedral cage structures consisting of a five-atom bulklike core filled inside reconstructed fullerene cages. They used this structural model to construct Si_{33}, Si_{39}, and Si_{45}. Sun *et al.* [17] studied a $Si_6@Si_{30}$ endohedral fullerene structure for Si_{36} using a first-principles method. For comparison we also included these three structures in our calculations. Within the present computational scheme, they are less energetically favorable than the present lowest-energy structures by 0.726, 0.392, and 3.419 eV for Si_{33}, Si_{36}, and Si_{39}, respectively. These results demonstrate that one has to be very careful to choose the optimal filling and/or cage combinations within the filled fullerene structural pattern. DFT-MD relaxation combined with DFT local minimization has proven to be an efficient way to find out the lowest-energy endohedral fullerene cages.

It is also interesting to investigate the stability of the medium-sized silicon clusters upon hydrogenation. One can define the formation energy of a hydrogenated silicon cluster from the difference between the total energy of Si_NH_{2M} and the sum of the total energies of Si_N and M times of the total energy of H_2 molecules. We found that the formation of hydrogenated silicon clusters is exothermic. For example, the computed formation energies for $Si_{31}H_8$ and $Si_{37}H_6$ are 4.761 and 3.534 eV, respectively. This is the same as the result of Ref. [33].

In Ref. [20], an empirical rule for the filling and/or cage ratio (m/n) of a filled fullerene cage $Si_m@Si_n$ was summarized on the basis of the results of GA global optimizations for Si_N ($N=27-39$) clusters. Considering a fullerene cage with $n=26+2x$ atoms, the upper and lower limits for the number m of filling atoms should be between $3+x$ and x. For the Si_N clusters ($30 \leqslant N \leqslant 39$) studied in this work, the lowest-energy filled cages fit well with that rule. For example, in the case of $n=32$, m can be 3–6, corresponding to combinations of $Si_3@Si_{32}$ for Si_{35} to $Si_6@Si_{32}$ for Si_{38}.

More recently, another empirical rule for the optimal filling and/or cage has been proposed within a simple space-filling picture [18,19]. In this model, the number m of the atoms filled inside a spherical-like fullerene cage with n atoms (in the range of $n=26-60$) can be expressed by a simple function as

$$m \approx 0.0051n^2 + 0.03071n - 1.5525. \quad (1)$$

For $30 \leqslant n+m \leqslant 39$, Eq. (1) predicts $m \approx 3.02$, 3.26, 3.50, 3.75, 4.00, 4.26, 4.52, 4.78, 5.05, and 5.32, respectively,

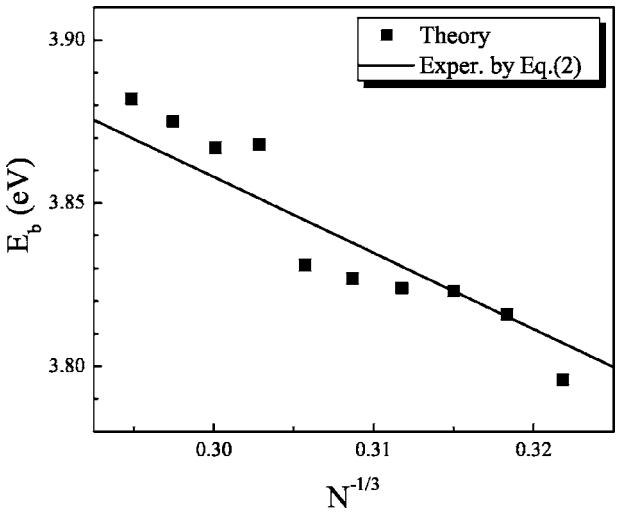

FIG. 2. Binding energy per atom (E_b) of medium-sized Si_N ($30 \leqslant N \leqslant 39$) clusters as a function of the inverse of the cluster radius $N^{-1/3}$. The theoretical results (black squares) obtained for the lowest-energy structures are compared to experimental data given by Eq. (2). We used the bulk binding energy $E_b(\infty)=4.58$ eV from GGA calculations with a shift of −0.023 eV for a better coincidence.

fairly close to our present results as $m=2, 3, 4, 3, 4, 3, 4, 5, 6$, and 5. Especially for Si_{37} and Si_{38}, Eq. (1) predicts the optimal numbers of $m=4.78, 5.05$, while our present calculations obtained $m=5,6$ and previous results were $m=3,4$ [20]. The comparison between those computational results with the prediction by the empirical rule implies that the space-filling picture is valid in the size range we studied and that previous GA optimization within the TB model seems to underestimate the number of endohedral silicon atoms in the filled cages.

In previous experiments [24,25], it was found that the binding energies E_b per atom of Si_N clusters ($N \geqslant 25$) could be roughly described by

$$E_b(N) = E_b(\infty) - cN^{-1/3} \tag{2}$$

where $E_b(\infty)$ is the binding energy per atom for bulk silicon solid (experiment: 4.63 eV, DFT calculation at PBE-DND level: 4.58 eV [19]). For the medium-sized range with $25 \leqslant N \leqslant 70$, a coefficient $c=2.33\pm0.03$ eV [25] was obtained from the data by collision induced dissociation experiments [24]. In Fig. 2, we plot the computed binding energies per atom (E_b) for the lowest-energy structures of Si_N clusters ($30 \leqslant N \leqslant 39$) as a function of the inverse of cluster radius $N^{-1/3}$, along with the prediction by Eq. (2). First, the theoretical binding energy increases gradually with increasing cluster size, which is an essential requirement for identifying stable medium-sized clusters [20]. The theoretical trend for the increase of binding energy with cluster size agrees reasonably with the experiment given by Eq. (2).

In summary, DFT calculations have been performed to search the lowest-energy configurations for medium-sized Si_N ($30 \leqslant N \leqslant 39$) clusters within the filled fullerene structural pattern. For each size, silicon fullerene cages with different topological structures and those filled by a different number of silicon atoms have been constructed and optimized using molecular dynamic relaxation followed by numerical optimization, at the DFT level. For most cluster sizes, the energies of the lowest-energy fullerenes cage structures obtained in this work are usually lower than those obtained in previous theoretical calculations [20]. For Si_{37} and Si_{38} the optimal filling and/or cage combination are found to be $Si_5@Si_{32}$ and $Si_6@Si_{32}$, different from previously proposed ones ($Si_3@Si_{34}$ and $Si_4@Si_{34}$) in Ref. [20]. The present results agree well with an empirical space-filled model, which assumes spherical fullerene cages filled with atomic spheres. The computed binding energies for the lowest-energy configurations agree reasonably with experimental data. The present results indicate that one has to examine all the possible possibilities and to optimize them at a first-principle level in order to find the lowest-energy configuration of medium-sized silicon clusters within the structural pattern of filled fullerene cages.

ACKNOWLEDGMENTS

This work was financially supported by the National Natural Science Foundation of China (Grants No. 90206033, No. 10274031, No. 10474030, and No. 60478012), the Foundation for the Author of National Excellent Doctoral Dissertation of the People's Republic of China (Grant No. 200421).

[1] R. L. Johnston, *Atomic and Molecular Clusters* (Tylor & Francis, London, 2002).
[2] C. C. Arnold and D. M. Neumark, J. Chem. Phys. **99**, 3353 (1993).
[3] E. C. Honea, A. A. Shvartsburg, B. Pan, Z. Y. Lu, C. Z. Wang, J. G. Wacker, J. L. Fye, and M. E. Jarrold, Nature (London) **366**, 42 (1993).
[4] S. Li, R. J. Van Zee, W. Weltner, Jr., and K. Raghavachari, Chem. Phys. Lett. **243**, 275 (1995).
[5] K. Raghavachari and C. M. Rohlfing, J. Chem. Phys. **89**, 2219 (1988).
[6] Z. Y. Lu, C. Z. Wang, and K. M. Ho, Phys. Rev. B **61**, 2329 (2000).
[7] K. M. Ho, A. A. Shvartsburg, B. Pan, Z. Y. Lu, C. Z. Wang, J. G. Wacker, J. L. Fye, and M. E. Jarrold, Nature (London) **392**, 582 (1998).
[8] K. A. Jackson, M. Horoi, I. Chaudhuri, T. Frauenheim, and A. A. Shvartsburg, Phys. Rev. Lett. **93**, 013401 (2004).
[9] F. S. Khan and J. Q. Broughton, Phys. Rev. B **43**, 11754 (1991).
[10] J. Song, S. E. Ulloa, and D. A. Drabold, Phys. Rev. B **53**, 8042 (1996).

[11] B. X. Li and P. L. Cao, J. Phys.: Condens. Matter **13**, 10865 (2001).
[12] Z. F. Chen, H. J. Jiao, G. Seifert, A. H. C. Horn, D. K. Yu, T. Clark, W. Thiel, and P. V. R. Schleyer, J. Comput. Chem. **24**, 948 (2003).
[13] E. Kaxiras, Phys. Rev. Lett. **64**, 551 (1990); E. Kaxiras, and K. Jackson, *ibid.* **71**, 727 (1993).
[14] D. A. Jelski, B. L. Swift, T. T. Rantala, X. F. Xia, and T. F. George, J. Chem. Phys. **95**, 8552 (1991).
[15] J. Pan and M. V. Ramakrishna, Phys. Rev. B **50**, 15431 (1994); M. V. Ramakrishna and J. Pan, J. Chem. Phys. **101**, 8108 (1994).
[16] M. Menon and K. R. Subbaswamy, Phys. Rev. B **51**, 17952 (1995).
[17] Q. Sun, Q. Wang, P. Jena, S. Waterman, and Y. Kawazoe, Phys. Rev. A **67**, 063201 (2003).
[18] J. L. Wang, X. L. Zhou, G. H. Wang, and J. J. Zhao, Phys. Rev. B **71**, 113412 (2005).
[19] J. J. Zhao, J. L. Wang, J. Jellinek, S. Yoo, and X. C. Zeng, Eur. Phys. J. D **34**, 35 (2005).
[20] S. Yoo, J. J. Zhao, J. L. Wang, and X. C. Zeng, J. Am. Chem. Soc. **126**, 13845 (2004).
[21] I. Rata, A. A. Shvartsburg, M. Horoi, T. Frauenheim, K. W. Michael Siu, and K. A. Jackson, Phys. Rev. Lett. **85**, 546 (2000).
[22] S. Yoo, X. C. Zeng, X. Zhu, and J. Bai, J. Am. Chem. Soc. **125**, 13318 (2003).
[23] M. F. Jarrold and V. A. Constant, Phys. Rev. Lett. **67**, 2994 (1991); R. R. Hudgins, M. Imai, M. F. Jarrold, and P. Dogourd, J. Chem. Phys. **111**, 7865 (1999).
[24] M. F. Jarrold and E. C. Honea, J. Phys. Chem. **95**, 9181 (1991).
[25] T. Bachels and R. Schafer, Chem. Phys. Lett. **324**, 365 (2000).
[26] K. Fuke, K. Tsukamoto, F. Misaizu, and M. Sanekata, J. Phys. Chem. **99**, 7807 (1993).
[27] M. A. Hoffmann, G. Wrigge, B. von Issendorff, J. Muller, G. Gantefor, and H. Haberland, Eur. Phys. J. D **16**, 9 (2001).
[28] U. Ray and M. F. Jarrold, J. Chem. Phys. **94**, 2631 (1991). M. F. Jarrold, Y. Ijiri, and U. Ray, *ibid.* **94**, 3607 (1991).
[29] URL: http://www.cochem2.tutkie.tut.ac.jp/Fuller/fsl/fsl.html
[30] M. D. Segall, P. J. D. Lindan, M. J. Probert, C. J. Pickard, P. J. Hasnip, S. J. Clark, and M. C. Payne, J. Phys.: Condens. Matter **14**, 2717 (2002).
[31] B. Delley, J. Chem. Phys. **92**, 508 (1990); **113**, 7756 (2000).
[32] J. P. Perdew, K. Burke, and M. Ernzerhof, Phys. Rev. Lett. **77**, 3865 (1996).
[33] V. Kumar and Y. Kawazoe, Phys. Rev. Lett. **90**, 055502 (2003).